

# CFRP structure for the LBT instrument LINC-NIRVANA

Ralf-Rainer Rohloff<sup>\*a</sup>, Norbert Münch<sup>a</sup>, Armin Böhm<sup>a</sup>, Wolfram Schlossmacher<sup>b</sup>,  
Carsten Schöppinger<sup>c</sup>, Hartmut Neugeboren<sup>c</sup>, Henrik Wittke<sup>c</sup>,  
Henning Wichmann<sup>c</sup>

<sup>a</sup>Max-Planck-Institut für Astronomie (MPIA), Königstuhl 17, 69117 Heidelberg, Germany

<sup>b</sup>Ingenieurbüro Schlossmacher, Valerystr. 16a, 85716 Unterschleissheim, Germany

<sup>c</sup>INVENT GmbH, Christian-Pommer-Str. 34, 38112 Braunschweig, Germany

## ABSTRACT

This paper describes the development of a Carbon Fiber-Reinforced Plastics (CFRP) structure for the interferometric instrument LINC-NIRVANA (LN) at the Large Binocular Telescope (LBT) Arizona, USA. This structure carries all components between the two “bent” Gregorian foci of the individual telescopes necessary to combine the light of the two arms coherently.

Especially developed for aerospace and defence, CFRP materials now find widespread use across a number of other applications where their special properties are beneficial. We will profit in LN from the good rigidity, high strength, low thermal expansion, low mass and high damping properties of CFRP.

An extended Finite Element Analysis was performed to simulate the properties of the structure for different telescope positions and different temperatures.

We built a 560 mm x 550 mm x 385 mm test piece of the LN optical bench for flexure tests to confirm the results of the Finite Element Analysis.

The complete LN instrument with a mass of 7.5 tons will be mounted at a tilting unit to simulate the different telescope positions.

Keywords: CFRP, Carbon Fiber, Optical Bench, Telescope Structures

## 1. INTRODUCTION

The LN instrument mounted at the LBT is a Fizeau interferometer (see [1] for more information about LN). The wavefronts interfere in the focal plane, not in the pupil plane. Fizeau imaging works best with compact arrays of telescopes, that is, configurations in which the separation of the mirrors is comparable to their diameter. At the LBT the two primary mirrors with a diameter of 8.4 m and separation of 23 m share a common steerable mount. The interferometric instrument is mounted directly at the telescope structure which reduces the number of reflections before the radiation enters the beam combiner. The instrument has the same environmental conditions as the telescope and non-controlled laboratory conditions like most ground-based interferometers of the coaxial or pupil-plane configuration [2]. Vibrations and thermal changes can impair the performance of an interferometric instrument. Therefore, we decided to use CFRP with a low thermal expansion coefficient and high damping properties despite the higher costs compared to steel or Aluminium.

The installation of bigger Aluminium or steel components at the CFRP optical bench can be a problem due to the thermal mismatch between the different materials. We designed special thermal compensations to avoid thermal stresses and also used CFRP as structural material for these components.

Due to the common use of CFRP in the sporting goods, aerospace and defence industry several providers are on the market, however it is very important to have a partner with a good theoretical background concerning the design of CFRP structures.

- [rohloff@mpia.de](mailto:rohloff@mpia.de); phone +49-6221-528310

## 2. LINC-NIRVANA STRUCTURAL DESIGN AND FEM-ANALYSIS

### 2.1. Design

The mounting structure for the LN instrument of the LBT has been developed and manufactured by INVENT GmbH, Braunschweig, Germany. The MPIA was supported by the Ingenieurbüro Schlossmacher, Unterschleissheim, Germany. For the development of the optical bench it was necessary that design and calculation (structural analysis) occur simultaneously.

Figure 1 shows the LN instrument mounted on the LBT instrument platform. The instrument does not use the rotating instrument adapters, it is fixed on two rails. The LN mounting structure is composed of the following main parts: optical bench, substructure and base frame.

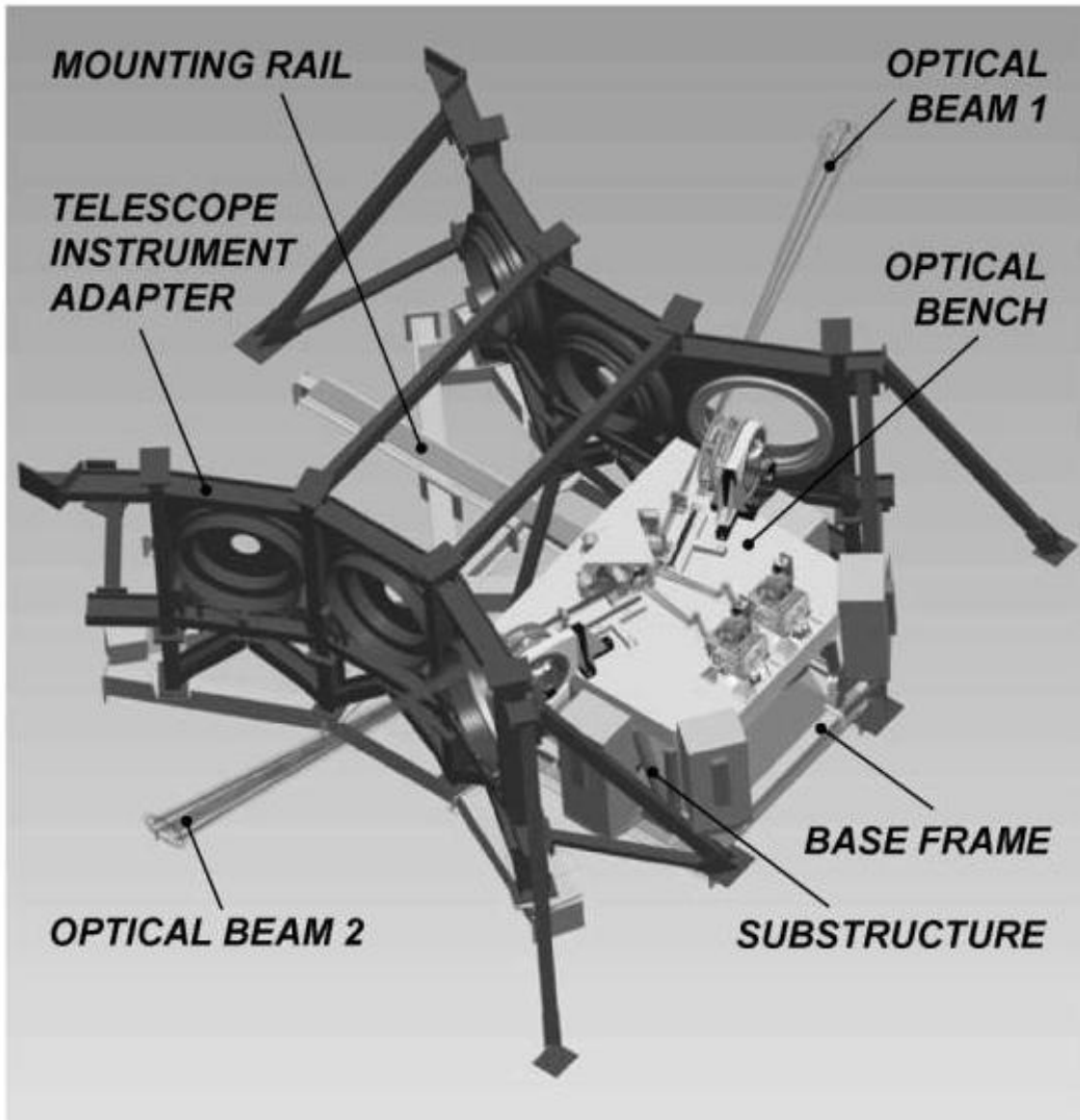


Figure 1: Model of the LN instrument mounted at the LBT instrument platform

The key requirements for the structural elements of the mounting structure are:

- high stiffness – minimum bending of structure due to telescope movement
- geometrical accuracy – positioning of optical and mechanical components at the optical bench with minimized adjustments
- high thermal stability – minimize mechanical changes due to temperature variations between day and night and between different seasons
- high damping properties – damping of internal (e.g. moving components, motors at the instrument) and external (e.g. telescope, wind) vibrations
- minimum weight – better handling properties

The optical bench consists of CFRP sandwich faces, interior CFRP-laminates, Aluminium inserts and Aluminium honeycombs.

The main parts of the substructure are CFRP-struts with glued fittings (CFRP-inserts) and bearing blocks of steel. Details for the design of the CFRP-struts of the substructure are shown in figure 2.

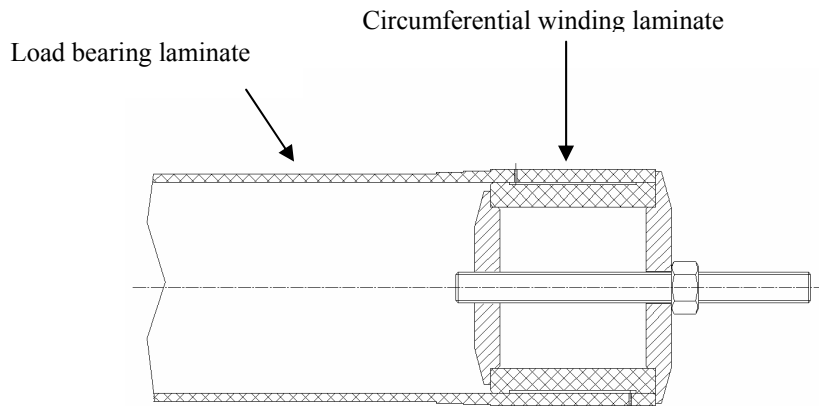


Figure 2: Design of the CFRP-struts

The connection substructure/optical bench has been realized by using bearing blocks (see figure 3). Above the sites of the connection, various inserts have been placed in the interior of the mounting platform. More inserts for loads up to 100 kg are integrated at the top of the optical bench. A view of an insert for heavy load and a cut through the optical bench is shown in figure 4.

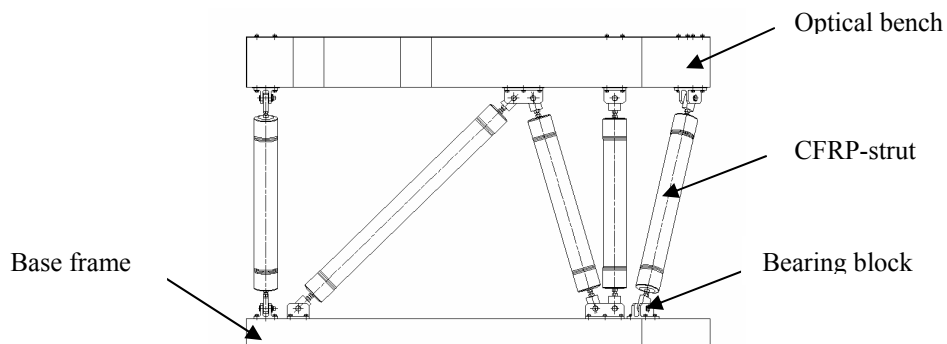


Figure 3: Connection between optical bench and CFRP-struts

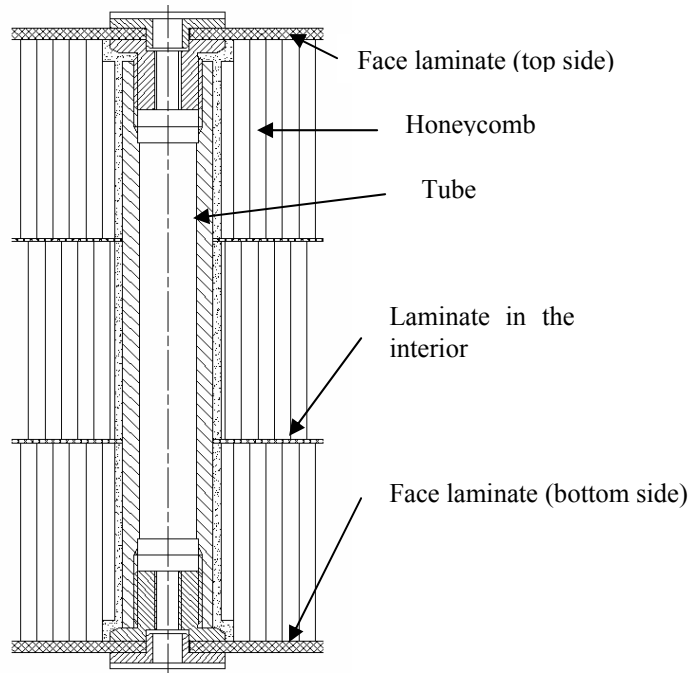


Figure 4: Insert for heavy load

The main focus of the FEM analysis is the calculation of the deformations or the displacements  $u_x$ ,  $u_y$  and  $u_z$ , respectively, of the optical bench. The deformations depend on the given load cases. The FEM-analysis distinguishes between the load cases “self-weight” and “thermal load” case. For the “self-weight” load case, the weight of substructure, mounting platform and various instruments are taken into account. Additionally, the different positions in dependence on the angle  $\alpha$  in the range  $0^\circ \leq \alpha \leq 60^\circ$  have to be taken into consideration (the angle  $\alpha$  describes the rotation around the y-axis). For the “thermal load” case, a temperature difference of  $\Delta T = 5$  K is assumed which is permissible during measuring periods of the telescope. For the load case “self-weight” the following masses were assumed:

- 1000 kg      Optical bench
- 1050 kg      Substructure
- 3060 kg      Instruments
- 450 kg        Cover and optional masses

(Note): Weight measurements upon completion of the optical bench and the substructure show slight differences from the values originally assumed. These differences do not affect the FEM-results in a significant manner.

## 2.2. Materials

The fibres CN60-60S und K63712 and the epoxy resin LY556/HY917/DY070 were chosen for the CFRP-laminates, e.g. for the sandwich faces and for the CFRP-struts. The carbon fibres CN60-60S (Granoc) and K63712 (Mitsubishi) show similar properties: both are UHM-fibres based on pitch. For the sandwich construction of the optical bench, Aluminium honeycombs ACG-1/4-4.8 (HEXCEL) are needed as core material.

The fibre volume content  $V_f$  of the sandwich faces, which are manufactured in vacuum technology, is in the range of  $57\% < V_f < 58\%$ . The smaller value  $V_f = 55\%$  is assumed for the analytical calculations and the FEM analysis.

Material properties (e.g. elasticity constants, coefficients of thermal expansion) are as follows:

$$\begin{aligned} E_{f||} &= 620 \text{ GPa}, \quad \alpha_{f||} = -1.4 \cdot 10^{-6} \text{ K}^{-1}, \\ \rho_f &= 2.12 \text{ g/cm}^3, \\ E_m &= 3.2 \text{ GPa}, \quad \nu_m = 0.35, \quad \alpha_m = 56 \cdot 10^{-6} \text{ K}^{-1}, \\ \rho_m &= 1.2 \text{ g/cm}^3 \end{aligned}$$

By using rule-of-mixtures relations and the relations of the classical lamination theory, various material properties or engineering constants have been estimated. For example, estimated properties of the almost quasi-isotropic face laminate are

$$\begin{aligned} E_x = E_y &= 131.9 \text{ GPa}, \quad G_{xy} = 36.1 \text{ GPa}, \\ \nu_{yx} &= 0.25, \quad \alpha_x = \alpha_y = -0.37 \cdot 10^{-6} \text{ K}^{-1}, \\ \rho_{CFK} &= 1.7 \text{ g/cm}^3 \end{aligned}$$

For the CFRP-struts, an angle ply laminate with  $\pm 16^\circ$ -orientations is assumed. For this laminate the following properties have been calculated:

$$\begin{aligned} E_x = E_y &= 204.5 \text{ GPa}, \quad G_{xy} = 26.2 \text{ GPa}, \\ \alpha_x &= -4.1 \cdot 10^{-6} \text{ K}^{-1}, \quad \rho_{CFK} = 1.7 \text{ g/cm}^3 \end{aligned}$$

Details concerning rule-of-mixtures relations and classical lamination theory: see [3] and [4].

### 2.3. FEM-Analysis

A view of the FEM-model is shown in figure 5.

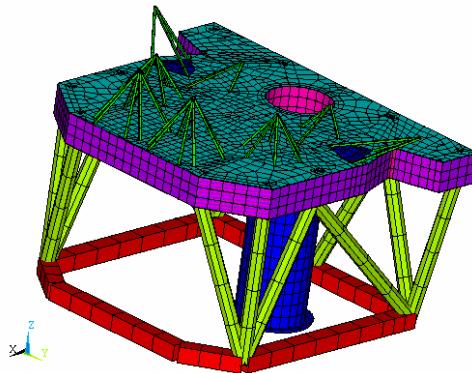


Figure 5: FEM-model of the optical bench

The dimensions of the optical bench are as follows:

- 3590 mm: maximum length (in x-direction)
- 4360 mm: maximum width (in y-direction)
- 382.5 mm: height (in z-direction)

The total height of the mounting structure (without base frame and instruments) is  $H = 2178$  mm. The instruments with the exception of the cryostat are replaced in the model by point masses which are connected with the optical bench by beam elements.

Results of the calculated displacements  $u_z$  for the load case “self-weight” and for  $\alpha = 0^\circ$  are shown in figure 6. The displacements  $u_x$  for the “thermal load” case are shown in figure 7.

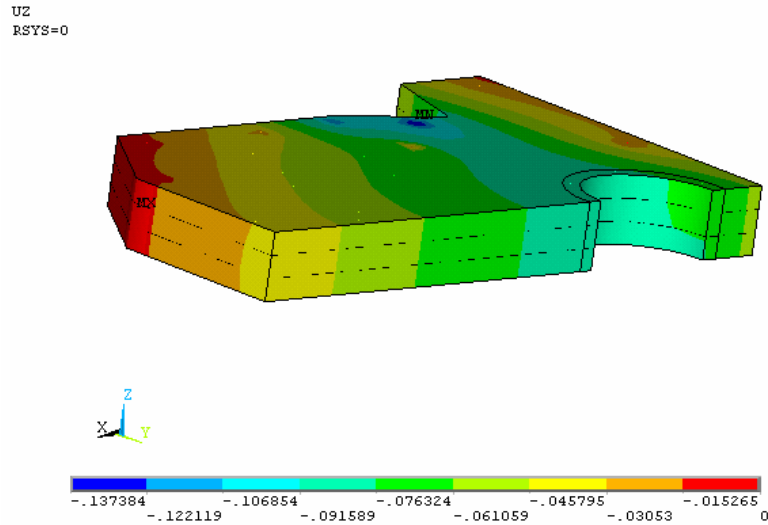


Figure 6: Mounting-Platform, displacements  $u_z$  for  $\alpha = 0^\circ$

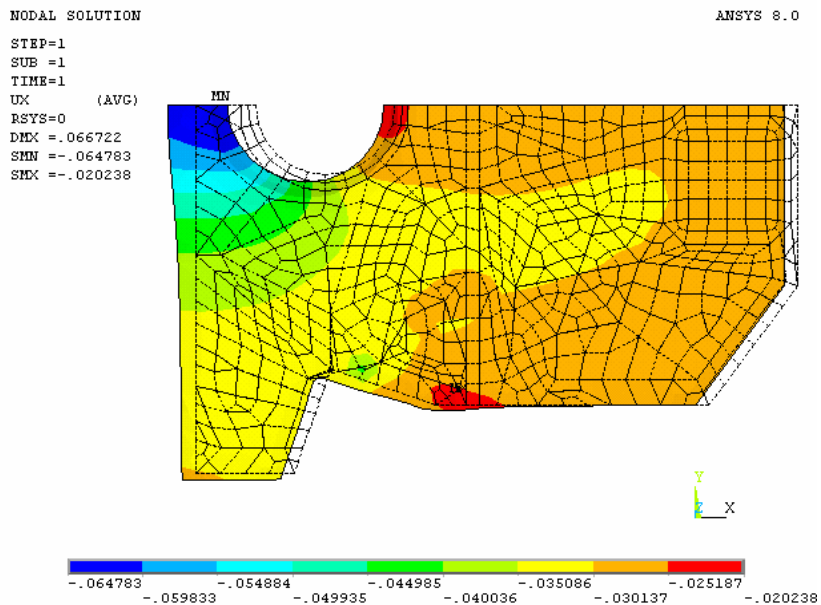


Figure 7: Mounting Platform, displacements  $u_x$  for  $\Delta T=5$  K

The amounts of the displacements must not exceed given limits:

$$|u_z| < 0,5 \text{ mm}, |u_x| < 0,5 \text{ mm}$$

Additionally, the amounts of differences of displacements between defined points must not exceed given limits when the angle  $\alpha$  changes. In some cases, the permissible value is only 0.01 mm. Such requirements depend on the path of rays between the interferometric instruments. These requirements are fulfilled when the thickness of the CFRP sandwich faces is 7 mm and the wall thickness of the CFRP-struts is 6.5 mm.

Due to the high stiffness required, the stresses in the CFRP laminates are low. High stresses are only found for the screws of the connecting elements between substructure and optical bench in the case of positions with  $\alpha \geq 60^\circ$ . For the stress analysis, rotation angles in the range  $60^\circ < \alpha < 90^\circ$  are taken into consideration, too. The  $90^\circ$  angle is only a storage and service position of the telescope.

#### 4. MANUFACTURING PROCESS

The substructure and the optical bench were manufactured independently. However, the CFRP-struts of the substructure were manufactured first.

For the manufacturing of the struts, winding technology and gluing have been used.

The manufacturing of the optical bench was carried out in several sub-steps. The first step was the manufacturing of the CFRP-layers (sandwich faces, laminates in the interior) by using vacuum technology. Afterwards the Aluminium honeycomb was glued. Figure 8 gives an example for the stepwise procedure. This figure shows a structure with two layers of Aluminium honeycomb which are separated by one CFRP-laminate.

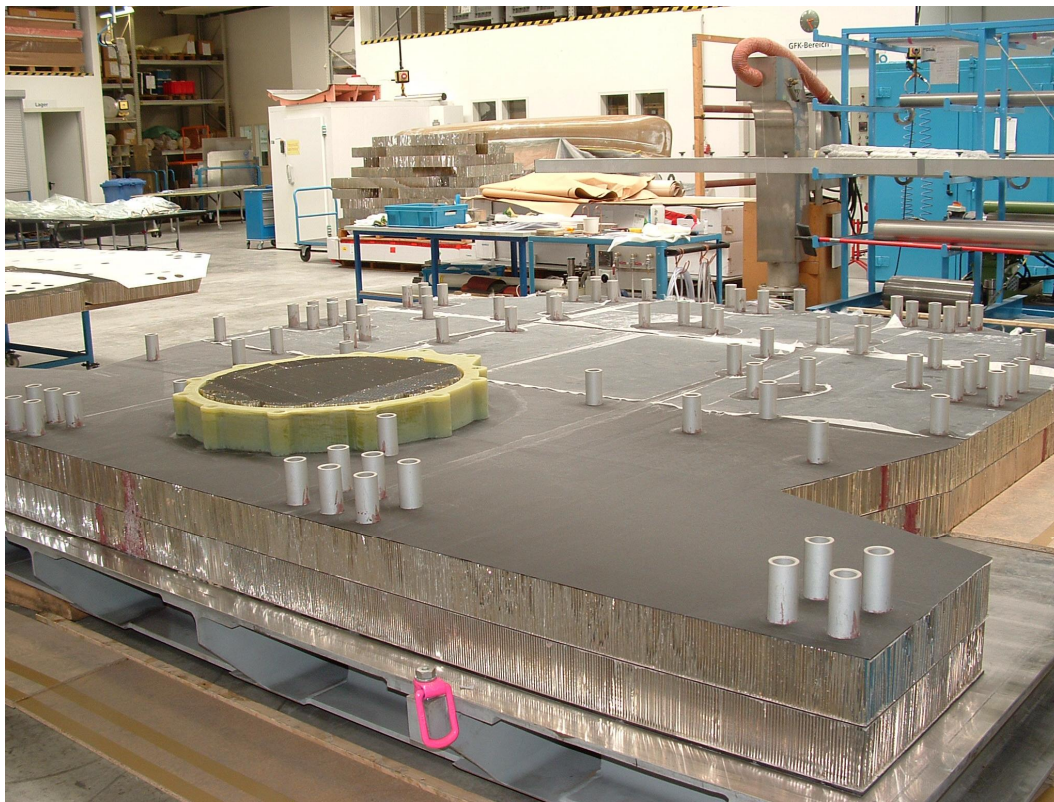


Figure 8: Manufacturing of the optical bench

Aluminium honeycomb and CFRP-layers were also glued by using vacuum technology. For the integration of the inserts for heavy loads, the space had to be cut out of the region of the Aluminium honeycomb first. Corresponding cut-outs are necessary in the case of the CFRP-layers. Inserts and honeycomb were glued by using corefiller poured into the space between them (compare figure 9).

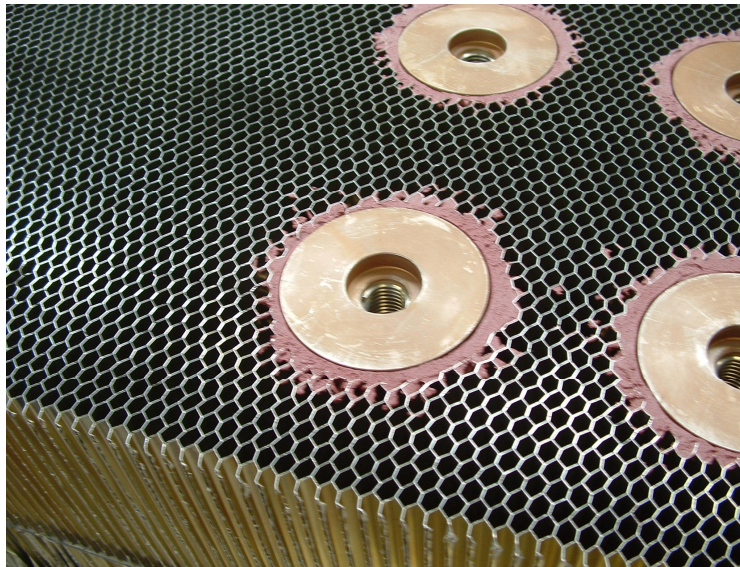


Figure 9: Connection between Aluminium honeycomb and inserts for heavy weights

Upon completion of CFRP-struts and mounting platform, both assemblies had been built up at INVENT GmbH before the single assemblies were subsequently transported to MPIA for finishing. The subsequent finishing consists of the integration of a great number of inserts for low loads at the topside of the optical bench, the milling of the inserts to a flatness accuracy of 0.05 mm (see figure 10) and the lacquered work. All metal parts (e.g. end fittings and inserts) are manufactured by the MPIA workshop.

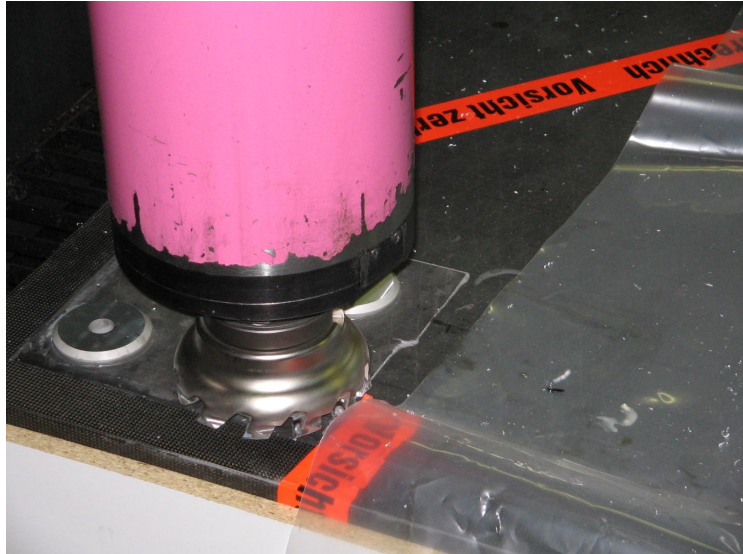


Figure 10: Milling of optical bench inserts

## 5. STRUCTURAL TESTS OPTICAL BENCH

### 5.1 Purpose and test set up

In order to validate the material properties, the numerical set ups and idealization method used for the FEM model of the optical bench, component test have been performed.

For this purpose, a honeycomb plate made from the same material batches of CFRP fibers and of Aluminium core as used for the optical bench.

The test sample was made in the size of 560 mm x 550 mm x 385 mm, showing the same laminate thickness and stacking sequence used for the optical bench. All edge surfaces were closed by edge filling compound and painted white to achieve light and unstructured surfaces for the optical Electronic Speckle Pattern Interferometry measurements (ESPI - contactless, optical method to detect deformations and strains at the entire surface). For load introduction and for constraining the test sample in a rigid test bench, the same type of inserts are used as in the CFRP optical bench. The tests were conducted under several load and constraint conditions to achieve representative data and to cover all possible load conditions of the CFRP optical bench (see table 1).

ID	LOAD	MEASURAND	SURFACE	DEVICE		Remarks	Sketch
				Primary	Secondary		
1.0	<b>Fx = 10 KN</b>						
1.1	Fx = 10 KN Load introduction at upper surface	$dx = f(y, FX)$	Top Surface XY	3D-ESPI	Strain Gage		
1.2	Fx = 10 KN Load introduction at upper surface	$dx = f(y, z, FX)$	Lateral Surface YZ	3D-ESPI	Strain Gage		
1.3	Fx = 10 KN Load introduction equally distributed between upper and lower surface	$dx = f(y, FX)$	Top surface XZ	3D-ESPI	Strain Gage	Evaluation of impacts due to unsymmetrical loading in load case 1.1	

Table 1: Load and Boundary Constraints

The integration of the test sample in the test bench is shown in figure 11.

Loads up to 38 kN are applied slowly by movements of the electro-hydraulic actuator ( $v = 0.01$  to  $0.1$  mm / s )



Figure 11: Sample mounted in test rig

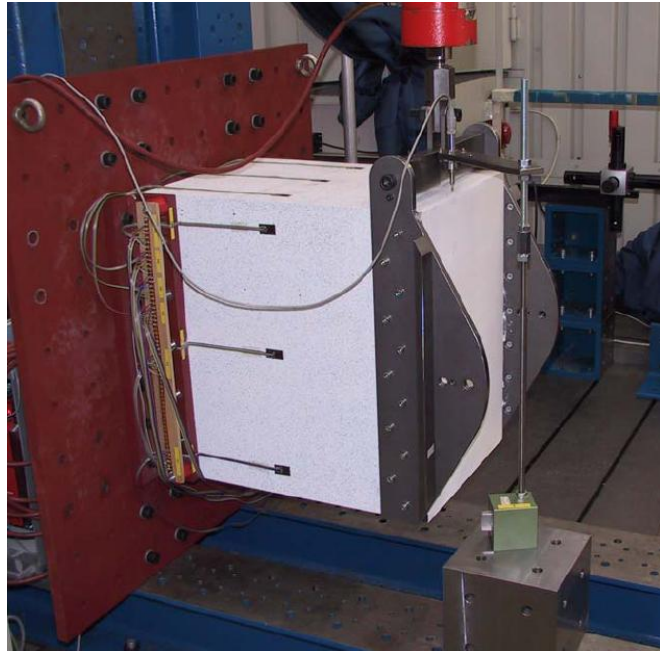


Figure 12: Strain gages and ESPI System

In addition, a separate FEM model was made reflecting size, load introduction and boundary conditions at the test sample.

Strains were measured by strain gages at selected locations and by ESPI (figure 12).

## 5.2 Discussion of results

The deformation measurements at the strain gages and of the ESPI both show a high degree of correlation with the analytical results (see figure 13 and 14).

Furthermore the strain measurements at the strain gages comply with the analytical results. The results are compared in table 2.

Reference	Strain	
	FEM	Strain Gages
Test No. 1.1	$\epsilon_1 = 0,043 \times 10^{-3}$	$\epsilon_1 = 0,038 \times 10^{-3}$
	$\epsilon_2 = -0,043 \times 10^{-3}$	$\epsilon_2 = -0,040 \times 10^{-3}$
Test No. 2.1	$\epsilon_1 = 0,065 \times 10^{-3}$	$\epsilon_1 = 0,077 \times 10^{-3}$
	$\epsilon_2 = -0,0145 \times 10^{-3}$	$\epsilon_2 = -0,023 \times 10^{-3}$
Test No. 3.1	$\epsilon_1 = 0,007 \times 10^{-3}$	$\epsilon_1 = 0,005 \times 10^{-3}$
	$\epsilon_2 = -0,033 \times 10^{-3}$	$\epsilon_2 = -0,032 \times 10^{-3}$

Table 2: Comparison of results of FEM and strain gages

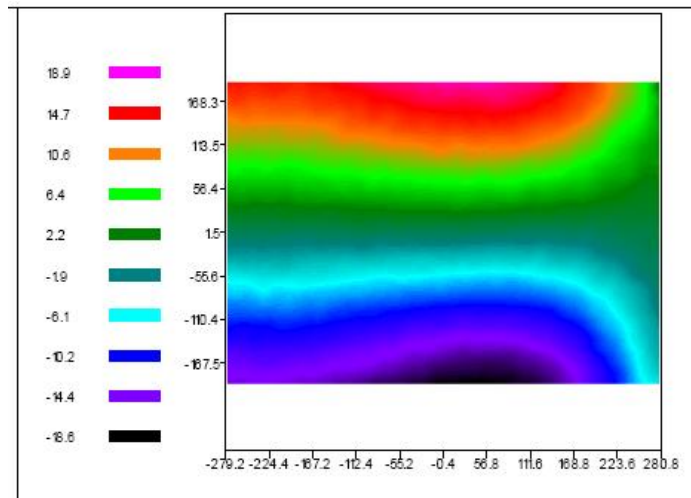


Figure 13: ESPI Deformation Plot for Test No. 1.3 ( $u_y = -18,6 \mu\text{m} \div 18,7 \mu\text{m}$ )

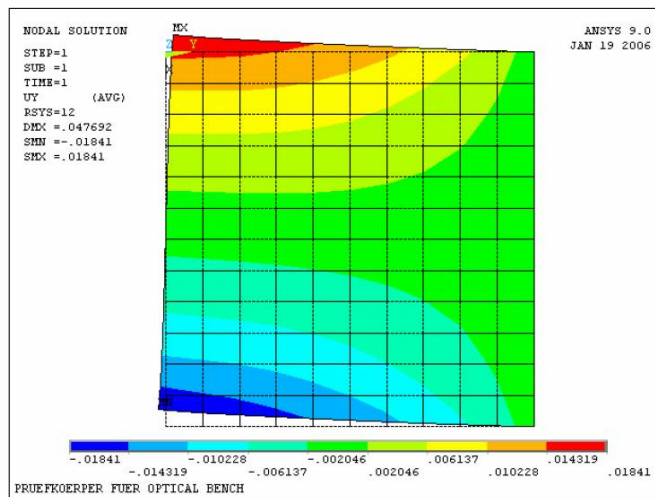


Figure 14: FEM Deformation Plot for Test No. 1.3 ( $u_y = -18,4 \mu\text{m} \div 14,3 \mu\text{m}$ )

The strain results from the ESPI are impacted by rigid body mode movements of the sample. In addition, calibration effects impact the strain results as the strain data are calculated by numerical derivation of deformation data.

### 5.3 Conclusions

The used type idealization and the numerical set ups for material properties in the FEM-model show excellent correlation with the results found in the component tests.

The analytical results found at the optical bench in terms of deformation and strain are regarded validated.

## 6. LAB INTEGRATION OF LINC-NIRVANA

Figure 15 shows the LN instrument support structure in the integration hall at MPIA. The structure is mounted at a tilt platform to simulate the telescope movement. We can move the LN instrument from  $0^\circ$  to  $90^\circ$  with the telescope simulator.

The bending of the structure at positions of interest will be measured by photogrammetry in each integration step. Additionally, the performance of the mounted components at different telescope positions must be examined.

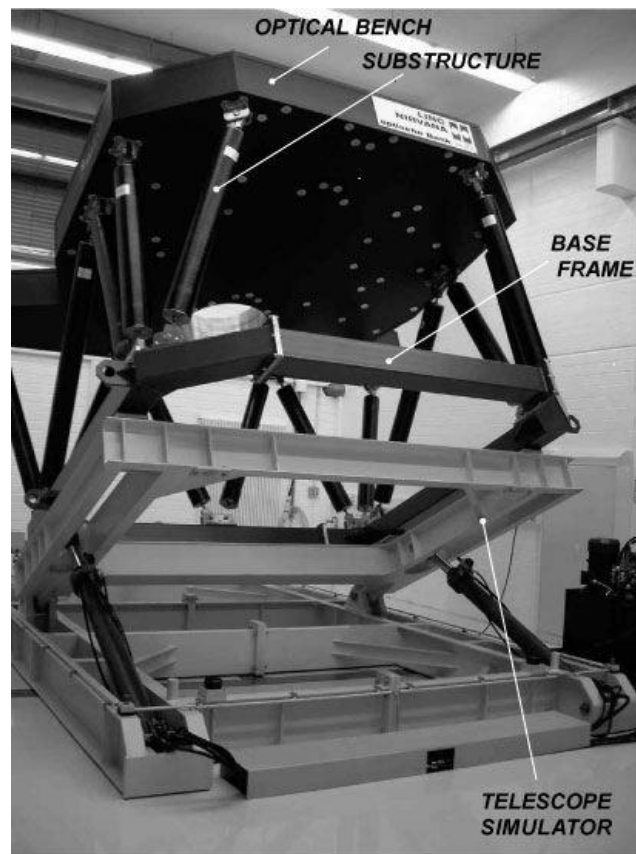


Figure 15: LN instrument support structure mounted at the telescope simulator

## 7. SUMMARY

We described in this paper the use of CFRP for the mounting structure of an astronomical instrument. Although the engineering and manufacturing efforts and costs are higher compared to other common materials, we can benefit from the excellent properties of CFRP.

Telescopes of the 8 m – 10 m class are in operation all over the world. Plans and first designs for telescopes with a mirror diameter of 30 m and more already exist. For financial reasons these new ground-based telescopes will be mainly made from metal, the use of CFRP for special points of interests, e.g. instrument mounting platforms, mirror support structures and other thermal or vibration sensitive parts is possible.

## REFERENCES

1. Tom Herbst et al., *Beyond the fringe: an update on the construction of LINC-NIRVANA, a Fizeau imaging interferometer for the LBT*, SPIE 6268-72, this conference, Orlando, 2006
2. LINC-NIRVANA consortium, *LINC-NIRVANA Final Design Review*, Heidelberg, 2005
3. Günther Niederstadt, *Ökonomischer und ökologischer Leichtbau mit faserverstärkten Polymeren*, Second Edition, expert Verlag, Renningen-Malsheim, 1997
4. Helmut Schürmann, *Konstruieren mit Faser-Kunststoff-Verbunden*, Springer-Verlag, Berlin, Heidelberg, 2005